



LAWRENCE
LIVERMORE
NATIONAL
LABORATORY

Continuously Variable Node Position in a High-Throughput Acoustofluidic Device

E. J. Fong, M. Bora, S. Y. Jung, A. Johnston, T.
Notton, L. S. Weinberger, M. Shusteff

July 23, 2014

MicroTAS
San Antonio, TX, United States
October 26, 2014 through October 30, 2014

Disclaimer

This document was prepared as an account of work sponsored by an agency of the United States government. Neither the United States government nor Lawrence Livermore National Security, LLC, nor any of their employees makes any warranty, expressed or implied, or assumes any legal liability or responsibility for the accuracy, completeness, or usefulness of any information, apparatus, product, or process disclosed, or represents that its use would not infringe privately owned rights. Reference herein to any specific commercial product, process, or service by trade name, trademark, manufacturer, or otherwise does not necessarily constitute or imply its endorsement, recommendation, or favoring by the United States government or Lawrence Livermore National Security, LLC. The views and opinions of authors expressed herein do not necessarily state or reflect those of the United States government or Lawrence Livermore National Security, LLC, and shall not be used for advertising or product endorsement purposes.

CONTINUOUSLY VARIABLE NODE POSITION IN A HIGH-THROUGHPUT ACOUSTOFLUIDIC DEVICE

Erika J. Fong^{1,2}, Mihail Bora¹, Seung-Yong Jung³, Amanda Johnston¹,
Timothy Notton⁴, Leor S. Weinberger^{3,4}, and Maxim Shusteff¹

¹Lawrence Livermore National Laboratory, USA, ²Boston University, USA,

³The Gladstone Institutes, ⁴University of California San Francisco, USA

ABSTRACT

Previously, we presented a novel approach to acoustofluidic device design that incorporates a thin wall to longitudinally subdivide the fluid channel, allowing high-quality particle focusing off the channel centerline [1]. Both parts of the channel participate in the acoustic resonance, allowing the resonance to be unconstrained by the dimensions of the separation channel. Here, we demonstrate continuously and arbitrarily tunable node position within a single device, using fluids of different densities in the secondary “bypass” channel.

KEYWORDS: acoustics, microfluidics, separation, ultrasound

INTRODUCTION

Acoustofluidic particle separators have developed to become an important class of high throughput microfluidic devices. Arbitrary node positioning within the microchannel has previously been demonstrated [2] using multi-mode superposition [3] with bulk acoustic waves (BAW) or phase [4,5] and frequency [6] control with surface acoustic waves (SAW). However, the majority of these devices use channels fabricated from PDMS, which dissipates acoustic energy, limiting the effectiveness of focusing. In all cases such devices have been limited to ~10 $\mu\text{L}/\text{min}$ maximum flow. Additionally, absorption and leaching of chemicals and gas permeability in PDMS presents challenges for certain applications. In contrast, our device is fabricated from silicon and glass which offer more efficient acoustic coupling into the sample fluid, and are more inert and robust. We anisotropically dry-etch fluidic channels into silicon, then anodically bond them to glass. The present work allows 1-2 orders of magnitude greater volumetric throughput and linear flow velocity.

EXPERIMENTAL

A 900 μm wide channel is subdivided by a 10 μm -thick silicon wall placed 300 μm from one edge. A PZT transducer glued to the chip drives the full-wave (2nd harmonic) resonance for the full 900 μm width. Figure 1a shows a schematic of the device and cross-sectional sketches of the sound pressure field with different fluids filling the bypass channel. We used ethanol, water and glycerol as bypass fluids to allow a wide range of adjustment for the acoustic node position, since their sound speeds differ significantly (approximately 1015, 1530, and 1920 m/s at 43 °C for pure ethanol, water, and glycerol, respectively). With water, the pressure node is located approximately 75 μm from the wall in the separation channel, and fluids with faster and slower sound speeds shift the node farther from and closer to the wall, respectively. We have tested our device with water, phosphate buffered saline (PBS) and 70% (v/v) ethanol in the separation channel; however, any combination of sample and bypass fluid may be used regardless of compatibility, since they are separated by an impermeable wall. This enables tuning of the node position for unknown sample fluids.

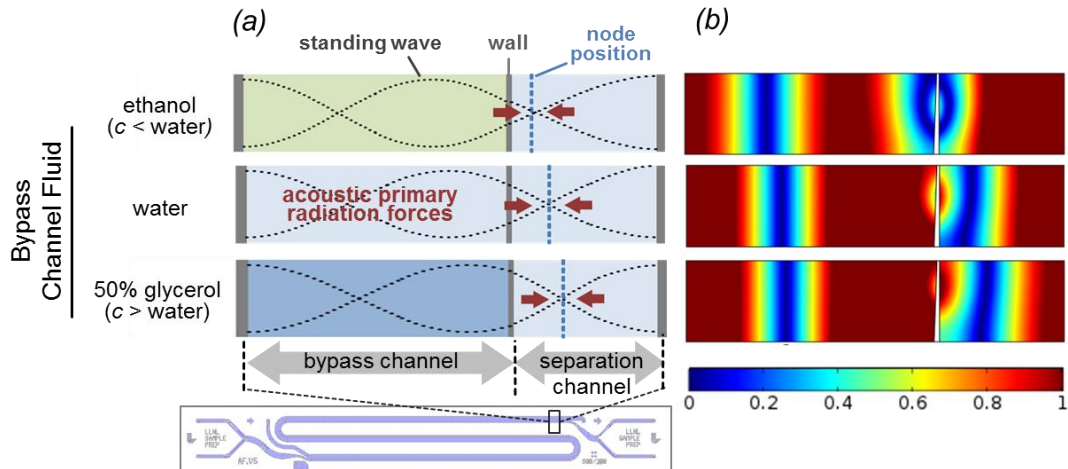


Figure 1: Schematic (a) and COMSOL simulation (b) of pressure amplitude at the second harmonic frequency with ethanol, water and 50% glycerol in the bypass channel and water in the separation channel. Sound waves in a fluid with lower sound velocity have a shorter wavelength, thus placing the node closer to the separation wall. In the COMSOL model, the wall thickness tapers from 6 μm at the top to 13 μm at the bottom, based on SEM images of the actual device as fabricated.

RESULTS AND DISCUSSION

Approximating the channel structure as a 1-D model, we calculated the predicted node positions and 2nd harmonic resonant frequencies analytically by using the relative speed of sound in each medium for water and 70% ethanol in the main channel. (Fig 2, lines). Using the acoustics-solid interaction module in COMSOL the fabricated microstructure was simulated in 2-D with various concentrations of ethanol and glycerol in the bypass channel and water or 70% ethanol in the separation channel to validate the 1-D model (dots). Device temperature is elevated by power dissipated in the piezo transducer; therefore, calculations and simulations were performed at 43°C using estimated physical properties for materials [7-12]. Figure 1b shows simulated pressure field amplitudes. Confirmatory focusing experiments were performed using 6 and 7 μm polystyrene microspheres in water, PBS and 70% ethanol using the technique described in [1], and experimental results are overlaid in Figure 2 as open markers. The simulation data shown in Figure 2 represent the minimum of the pressure amplitude across the channel centerline, however due to the taper of the wall the actual pressure node position varies across the height of the channel (Fig 1b), which may contribute to discrepancies between observed and predicted peak locations. When high concentrations of ethanol are in the bypass channel, the 2-D finite element model predicts that the pressure node will be split between the separation channel and bypass channel, and local minima in the pressure amplitude are observed on either side of the wall. (Fig 1b, ethanol in bypass). In these cases the experimentally found focusing position is along the wall. (Fig 2b, 100 and 90% ethanol in the bypass.) When 70% ethanol is in the main channel and 90% ethanol is in the bypass, the 2-D model does not predict splitting of the pressure node.

CONCLUSION

Using different fluid media in our subdivided-channel acoustofluidic device allows predictable shifting of the node position and the resonant frequency. Water and PBS behave similarly, which implies a device could be calibrated and used with most biological samples. Model and experimental results with 70% ethanol in the main channel show that the node position can be adjusted for a wide of materials in the separation channel.

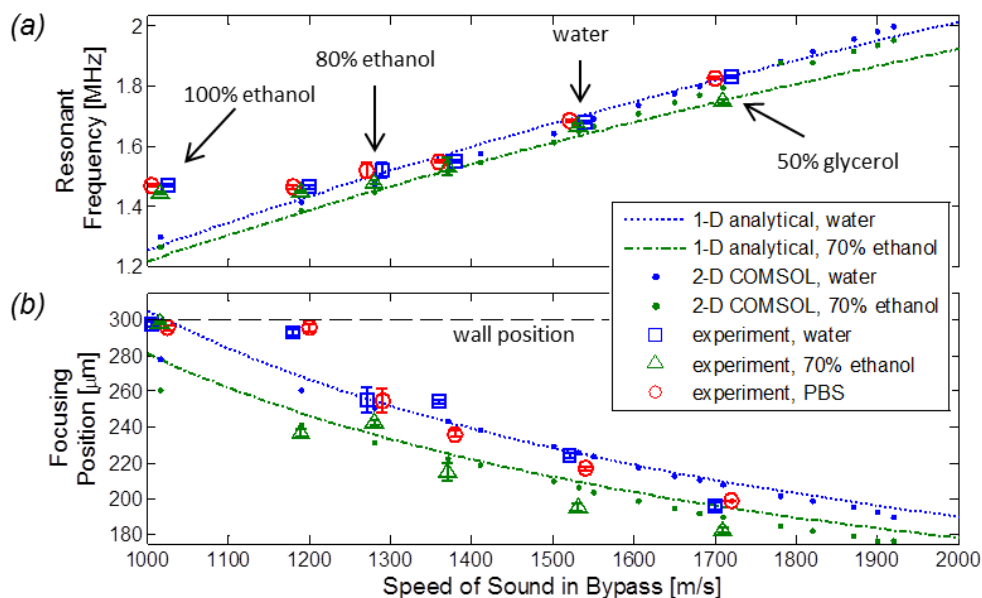


Figure 2: Analytical (lines), simulated (dots), and experimental (open symbols) results of using fluids with different sound velocities in the device. Legend indicates fluid in the separation channel. (a) Resonant Frequency. Error bars are the step size of the frequency sweep performed to determine resonant frequency, except when good focusing is observed over a large frequency range. In this case the error bars span this range. (b) Focusing Position. Error bars are one standard deviation of the position taken over 3 or more measurements at the resonant frequency. Black dashed line indicates wall position.

REFERENCES

- [1] E. J. Fong, A. C. Johnston, T. Notton, S.-Y. Jung, K. A. Rose, L. S. Weinberger, and M. Shusteff, *Analyst*, 2014, **139**, 1192–1200.
- [2] S. Kapishnikov, V. Kantsler, and V. Steinberg, *J. Stat. Mech. Theory Exp.*, 2006, **2006**, P01012.
- [3] P. Glynne-Jones, R. J. Boltryk, N. R. Harris, A. W. J. Cranny, and M. Hill, *Ultrasonics*, 2010, **50**, 68–75.
- [4] L. Meng, F. Cai, Z. Zhang, L. Niu, Q. Jin, F. Yan, J. Wu, Z. Wang, and H. Zheng, *Biomicrofluidics*, 2011, **5**, 044104–044104–10.
- [5] N. D. Orloff, J. R. Dennis, M. Cecchini, E. Schonbrun, E. Rocas, Y. Wang, D. Novotny, R. W. Simmonds, J. Moreland, I. Takeuchi, and J. C. Booth, *Biomicrofluidics*, 2011, **5**, 044107–044107–9.
- [6] S. Li, X. Ding, F. Guo, Y. Chen, M. I. Lapsley, S.-C. S. Lin, L. Wang, J. P. McCoy, C. E. Cameron, and T. J. Huang, *Anal. Chem.*, 2013, **85**, 5468–5474.
- [7] H. J. McSkimin and P. Andreatch, *Elastic Moduli of Silicon Vs. Hydrostatic Pressure*, Bell Telephone Laboratories, 1964.
- [8] *Physical Properties of Glycerine and Its Solutions*, Glycerine Producers' Association, 1963.
- [9] F. a. A. Fergusson, E. W. Guptill, and A. D. MacDonald, *J. Acoust. Soc. Am.*, 2005, **26**, 67–69.
- [10] M. Vatandas, A. B. Koc, and C. Koc, *Eur. Food Res. Technol.*, 2007, **225**, 525–532.
- [11] I. S. Khattab, F. Bandarkar, M. A. A. Fakhree, and A. Jouyban, *Korean J. Chem. Eng.*, 2012, **29**, 812–817.
- [12] N. A. Lange and J. A. Dean, *Lange's Handbook of Chemistry*, McGraw-Hill, 1973.

ACKNOWLEDGMENTS

This work performed under the auspices of the U.S. Department of Energy by Lawrence Livermore National Laboratory under Contract DE-AC52-07NA27344. LLNL-PROC-657658

CONTACT

* Maxim Shusteff, tel: 1-925-423-0733; Shusteff1@llnl.gov